J. Membrane Biol. 145, 87–98 (1995)

The Journal of
Membrane
Biology

Drug-transport and Volume-activated Chloride Channel Functions in Human Erythroleukemia Cells: Relation to Expression Level of P-Glycoprotein

F. Viana[1], K. Van Acker[2], C. De Greef[1], J. Eggermont[1], L. Raeymaekers[1], G. Droogmans[1], B. Nilius[1]

[1]Laboratory of Physiology, Catholic University of Leuven, Campus Gasthuisberg, B-3000 LEUVEN, Belgium
[2]Department of Hematology, Catholic University of Leuven, Campus Gasthuisberg, B-3000 Leuven, Belgium

Received: 31 August 1994/Revised: 28 December 1994

Abstract. The characteristics of volume-activated chloride currents, drug transport function and levels of P-glycoprotein (PgP) expression were compared between two human chronic erythroleukemia cell lines: a parental (K562) cell line and a derivative obtained by vinblastine selection (K562 VBL400). Parental K562 cells showed no detectable P-glycoprotein expression, measured at the protein level (immunofluorescence labeling with monoclonal antibodies), and had very low levels of MDR-1 mRNA expression (RT-PCR analysis), when compared with levels measured in K562 VBL400. Differences in Pgp-mediated transport were estimated by comparing the rates of Fluo3 accumulation. The higher drug-transport function of K562 VBL400 cells (e.g., lower Fluo3 accumulation) correlated with their elevated levels of MDR-1. The rate of dye transport was sensitive to verapamil but was not affected by the tonicity of the extracellular medium.

In contrast to the clear differences in transport function, the characteristics of chloride currents induced by cell swelling were indistinguishable between the two cell lines. Currents measured in the whole-cell configuration were outwardly rectifying, had a higher permeability to iodide than to chloride ($SCN^- > I^- > Cl^- >$ gluconate), were potently blocked by NPPB and were unresponsive to verapamil. The percentage of responding cells and the mean current density were nearly identical in both cell lines. In addition, activation of the volume-sensitive current was not prevented during whole-cell recordings obtained with pipettes containing high concentration of cytotoxic drugs (vincristine or vinblastine). These results do not lend support to the previously reported association between Pgp expression and volume-sensitive chloride channels, and suggest that a different protein is responsible for this type of chloride channel in K562 cells.

Correspondence to: F. Viana

Key words: Volume regulation — Multidrug resistance — Cancer cells — Chloride channels — MDR-1 gene.

Introduction

Chloride channels form a heterogeneous class of membrane proteins. Molecular cloning and sequencing have allowed the identification of several families of chloride transporting proteins. Furthermore, biophysical techniques permit discrimination between several types of chloride channels with respect to gating, anion selectivity, single channel conductance, pharmacology and regulation by intracellular factors (reviewed in Jentsch, 1993; Paumichl et al., 1993). Chloride channels are involved in a variety of cellular functions like transepithelial transport (Welsh, 1987; Frizzell & Halm, 1990; Welsh & Smith, 1993), inhibitory synaptic transmission (Bormann, Hamill & Sakman, 1987), cell division (Block & Mody, 1990), control of resting membrane potential in muscle cells (reviewed in Bretag, 1987), regulation of cell volume and control of intracellular pH (reviewed in Hoffmann and Simonsen, 1989; Grinstein & Foskett, 1990). Chloride channels may also function as mechanotransduction elements (Oike, Droogmans & Nilius, 1994).

The molecular identity of volume-activated chloride channels remains controversial. Studies in transfected 3T3 fibroblasts and lung epithelial cells strongly suggested that volume-activated chloride channels are associated with expression of P-glycoprotein (170 kD) (Valverde et al., 1992). This protein, the product of the MDR-1 gene, is a member of the ABC (ATP-binding cassette) superfamily of membrane transporters, that also includes the cystic fibrosis transmembrane conductance regulator. Expression of P-glycoprotein can confer multidrug resistance to eukaryotic cells by a mechanism that involves ATP-dependent extrusion of cytotoxic drugs

out of the cell (reviewed in Endicott and Ling, 1989). Additional experiments in MDR-1 transfected cells showed that P-glycoprotein-mediated transport and channel activity could be separated (Gill et al., 1992). A model was developed, suggesting that both activities of P-glycoprotein reflect two different, mutually exclusive, functional states of the protein (Gill et al., 1992). The interconversion between the two states is mediated by changes in the tonicity and by the availability of substrate. According to this proposal, incubation in hypotonic solution would switch the protein into its channel function mode. On the other hand, when the protein functions as transporter, channel function is excluded.

In contrast to aforesaid results, other studies in epithelial cell lines (Rasola et al., 1994) and Chinese hamster fibroblasts (Altenberg et al., 1994) did not reveal a clear correlation between the expression of a chloride conductance activated by cell swelling and the expression level of P-glycoprotein. Another putative chloride channel activated by changes in cell volume is the multidrug resistance-associated protein (MRP) (Jirsch et al., 1993). Like Pgp, MRP is also a member of the ATP-binding cassette transmembrane transporter superfamily (Cole et al., 1992). Finally, the chloride channel ClC-2 also has been shown to be activated by changes in cell volume when expressed in *Xenopus* oocytes (Gründer et al., 1992). However, the recent description of a native chloride channel activated by hypotonicity (Ackerman, Wickman & Clapham, 1994) and the identification of an endogenous swelling-induced chloride conductance regulatory protein in *Xenopus* oocytes (Paulmichl et al., 1992; Krapivinsky et al., 1994) complicates the interpretation of the aforesaid results. In a recent study, Nilius et al. (1994*c*) characterized a volume-activated chloride current in a large number of cell lines. They concluded that volume-activated chloride conductances are ubiquitously expressed in mammalian cells and that they share a lot of properties but also display pharmacological and regulatory differences. Collectively, these studies point to a possible diversity of volume-activated chloride channels.

The principal aim of this study was to investigate the possible relationship between volume-activated chloride channel function, drug transport function and P-glycoprotein expression in K562 cells, a human chronic erythroleukemia cell line. In addition we tested the hypothesis whether transport and channel functions of P-glycoprotein are interdependent.

Materials and Methods

Cell Culture

K562 (human chronic myelogenous leukemia cell line; ATCC CCL 243) and K562 VBL400 cells were grown in RPMI medium supplemented with 10% fetal calf serum. K562 VBL400 is a drug-selected cell line obtained by culturing K562 cells in the presence of progressively increasing doses of vinblastine up to 400 ng/ml as described (Van Acker, Van Hove & Boogaerts, 1993). Cultures were maintained at 37°C in a fully humidified atmosphere of 5% CO_2 in air. The culture medium was exchanged every 48 hr. Cells were detached by gentle shaking and either harvested for RNA isolation or, in case of electrophysiological experiments, reseeded on gelatin coated coverslips at a density of 1250–2500/cm^2. In the latter case, cells were kept in culture for at least 24 hr and a maximum of 7 days.

RT-PCR Analysis

Total RNA was extracted from a cell pellet containing 5×10^6 cells according to the Chomczynski method (1987) followed by a treatment with RNAse-free DNAse (Boehringer Mannheim). Total RNA (1 μg) was reverse transcribed into first strand cDNA using 200 ng of oligo$(dT)_{15}$ primers (Boehringer Mannheim) in 20 μl containing (mM) 50 Tris/HCl pH 8.3, 75 KCl, 3 $MgCl_2$, 1 DTT, 0.5 of each dNTP, 40 U RNasin (Promega) and 200 U Moloney-murine leukemia virus (M-MLV) reverse transcriptase (RT) (Life Sciences BRL). A blank RT reaction containing all components except the M-MLV-RT was performed in parallel. 3 μl aliquots of the RT+ and RT− first strand reaction mixture were used for PCR amplification in a 50 μl reaction containing 200 μM dNTPs, 0.5 μM primers and 2.5 units thermostable Tub DNA polymerase (Amersham Life Science) and the commercially supplied low Mg^{2+} buffer. Samples were denatured at 94°C for 2 min followed by 32 cycles of 1 min at 94°C, 1 min at 63°C and 1 min at 72°C. PCR products were separated on a 6% nondenaturing polyacrylamide gel and visualized by ethium bromide staining. To label the PCR products, 5 μl of the first PCR mix was diluted into a fresh 50 μl PCR mix containing 2.5 μCi of dCTP[α-^{32}P] and amplified for 10 additional cycles. A nondiscriminatory primer pair that coamplifies human MDR-1 and MDR-2 fragments was used. The presence of MDR-1- and/or MDR-2-specific fragments was determined by digesting aliquots of the 265 nt MDR-1/2 ^{32}P-PCR products with Hinf I. Hinf I products of 182 and 83 nt are MDR-1-derived, while 138 and 127 nt Hinf I bands correspond to MDR-2. Cut and uncut samples were run on a 6% nondenaturing polyacrylamide gel. The dried gels were processed on a PhosphorImager (Molecular Dynamics, Sunnyvale, California). The following primers were used to amplify MDR fragments: MDR-sense: TGCCTATGGAGACAACAGCCGGGT; MDR-reverse: GTCCAGGGCTTCTTGGACAACCTT.

RT-PCR analysis for actin mRNAs was performed to check the quality of the RNA samples. Actin primers were isoform-unspecific allowing amplification of α-, β- and γ-actin: sense primer: GCTGACAGGATGCAGAAGGAG; anti-sense primer: GATCCACATCTGCTGGAAGG. The annealing temperature for this primer set was 55°C.

FACS Analysis of Pgp Expression

Cell surface expression of Pgp was evaluated by immunofluorescence using a FACS flow cytometer (Becton Dickinson). Pgp expression was detected with MRK16, a monoclonal antibody directed against an extracellular epitope of MDR-1 Pgp (Hamada & Tsuruo, 1987). MRK16 was a kind gift from Dr. T. Tsuruo, Cancer Chemotherapy Center, (Tokyo). An isotypic monoclonal antibody (isotype IgG2a) was used as a control antibody for nonspecific binding. Cells (0.5×10^6 per tube) were washed once in phosphate buffered saline (PBS), pelleted and resuspended in blocking buffer (1% bovine serum albumin, 5% normal mouse serum, 10% human AB serum in PBS). MRK16, or the control isotypic antibody, was added to a final concentration of 20 μg/ml and

incubated for 30 min at 4°C. Cells were then washed twice with PBS and incubated with a secondary antibody (phyco-erythrin conjugated rat anti-mouse) for 30 min. Cell labeling was analyzed on a FACS flow cytometer with a minimum of 10^4 events being counted.

Fluo3 Transport Assay

Cells were harvested and resuspended in Hanks Buffered Saline Solution (HBSS) without Ca^{2+} or Mg^{2+} at a concentration of 2×10^5 cells per ml. Cells were aliquoted in 200 μl and prewarmed at 37°C for 10 min. 200 μl HBSS containing 8 μM Fluo3-AM (Molecular Probes) was then added to the cells. When necessary, the Fluo3-AM solution contained 40 μM verapamil to block MDR-1 mediated transport. Uptake measurements were started immediately after the addition of Fluo3-AM. Accumulation of Fluo3 in the cells was followed by monitoring the cell-associated mean fluorescence (excitation wavelength = 488 nm; emission wavelength = 525 nm) with a FACS flow cytometer during a 1 min-time interval. The Fluo3 uptake rate was expressed as the change in mean channel fluorescence per unit of time. To examine the effect of extracellular hypotonicity on transport activity, 120 μl of cells resuspended in HBSS were diluted to 200 μl by adding either 80 μl distilled H_2O (40% reduction in osmolarity) or 80 μl of HBSS (isotonic condition). Fluo3-AM (8 μM in 200 μl hypotonic HBSS (40% reduction in osmolarity)) or isotonic HBSS was added as required. When necessary, this solution contained 40 μM verapamil. Uptake measurements were started immediately after the addition of Fluo3-AM. This corresponded to a time interval of 30 sec between the reduction of the tonicity of the cell suspension and the beginning of the assay. In some experiments, there was a time interval of 3 min between the hypotonic stimulus and the beginning of the transport assay.

Electrophysiology

A detailed description of our recording methods has been provided elsewhere (Nilius et al., 1994*a*). In most experiments, whole-cell membrane currents were measured using conventional ruptured patches. Series resistance compensation was used routinely and amounted to 40–60% of total access resistance. In some experiments, the nystatin-perforated-patch technique was used instead (Horn & Marty, 1988). Currents were monitored with an EPC-7 (List Electronic, Germany) patch clamp amplifier and sampled at 4 msec intervals (2048 points per record, filtered at 100 Hz). The voltage protocol consisted of 1.2 sec step to −80 mV starting from a holding potential of 0 mV, followed by a step of 0.4 sec to −150 mV and a 5.2 sec linear voltage ramp to +100 mV and a return to the holding potential. In some experiments, a prepulse to −100 mV (50 msec) was followed by a 1-sec ramp to +100 mV. These two protocols were applied every 10 to 15 sec and have the advantage that complete *I-V* curves can be continuously generated during the experiment and that activation of the swelling-induced current can be tested at any membrane potential. The *I-V* relationship of the volume-activated current and its reversal potential was obtained from difference currents, measured during the voltage ramp in isosmotic and hyposmotic solutions. The relative permeability to different anions was estimated by the shift in reversal potential of the swelling-sensitive current, according to the following expression:

$$\Delta E_{rev} = E_{x^-} - E_{Cl^-} = RT/zF \ln (P_{x^-} \cdot [X^-]_o / P_{Cl^-} \cdot [Cl^-]_o)$$

Solutions

The standard isosmotic solution was (in mM): 105 NaCl, 0.5 $MgCl_2$, 1.3 $CaCl_2$, 10 HEPES, 70 D-Mannitol (275 mOsm/l). Hypertonic external solution contained 120 mM D-mannitol. Cell swelling (hyposmotic external solution) was induced by omitting D-mannitol from the standard external solution (*see* Diaz et al., 1993). During anion substitution experiments 105 mM NaCl was replaced by the same concentration of the sodium salt of iodide, gluconate and thiocyanate. All solutions were adjusted to pH 7.4 with Tris. Osmolarity of all solutions was measured with a vapor pressure osmometer (Wescor, Utah).

The standard pipette (internal) solution was made up in Milli-Q water (Millipore) and contained (in mM): 100 K-Aspartate, 40 KCl, 2 $MgCl_2$, 4 Na_2-ATP, 10 HEPES, 0.1 EGTA buffered to pH 7.2 with KOH, (285 mOsm/l). In a separate series of experiments 250 μM vinblastine or 250 μM vincristine were added to the standard internal solution. During those experiments, recordings were alternated with pipettes containing standard internal solution. In 10 cells, 100 mM Cs-Aspartate replaced 100 mM K-Aspartate in the pipette. The composition of the K^+-free internal solution consisted of (in mM): 105 NMDG, D-Mannitol 70, 1 $MgCl_2$, 2 Na_2-ATP, 10 HEPES, 0.1 EGTA, buffered to pH 7.2 with HCl. For perforated-patch experiments, a stock of nystatin (5 mg in 50 μl dimethylsulfoxide) was suspended by sonication in the standard internal solution at a final concentration of 500 μg/ml. Recording pipettes had resistances between 3–9 MΩ when filled with internal solution. The ground reference electrode was an agar bridge filled with 150 mM KCl. The liquid junction potential between the standard pipette solution and the isosmotic bath solution was −3 mV (pipette negative). The relative junction potentials of anion-substituted external solutions had the following values (in mV): I^-, 0; SCN^-, 0; gluconate, −3. These values were obtained by measuring the shift in zero current voltage of the EPC-7 amplifier when switching between the various solutions. These potentials were not corrected in the figures, but were corrected in the description of reversal potentials and relative permeabilities throughout the text.

Experiments were performed at room temperature (20–22°C). The chloride channel blocker 5-nitro-2-(3-phenylpropylamino)-benzoic acid (NPPB) was purchased from RBI (Natick, MA). All other drugs were from Sigma.

Statistics

Pooled data are given by mean ± SE of the mean (n, number of observations). For statistical comparisons Student's t test was used. Differences were considered significant when P was less than 0.05.

Results

Expression of MDR-1 Pgp in K562 and K562 VBL400 Cells

Expression of MDR-1 in K562 and K562 VBL400 cells, a vinblastine-selected derivative of K562, was examined at the RNA level by Reverse-Transcriptase-Polymerase Chain Reaction (RT-PCR) and at the protein level by immunofluorescence using a Fluorescence Activated Cell Scanner (FACS). For the RT-PCR analysis, total RNA was reverse transcribed with oligo-dT primers into first strand cDNA and cDNA aliquots were then amplified using a nondiscriminatory primer pair that amplifies human MDR-1 and MDR-2 cDNAs. Subsequent digestion of the 265 nucleotide MDR-1/2 PCR product

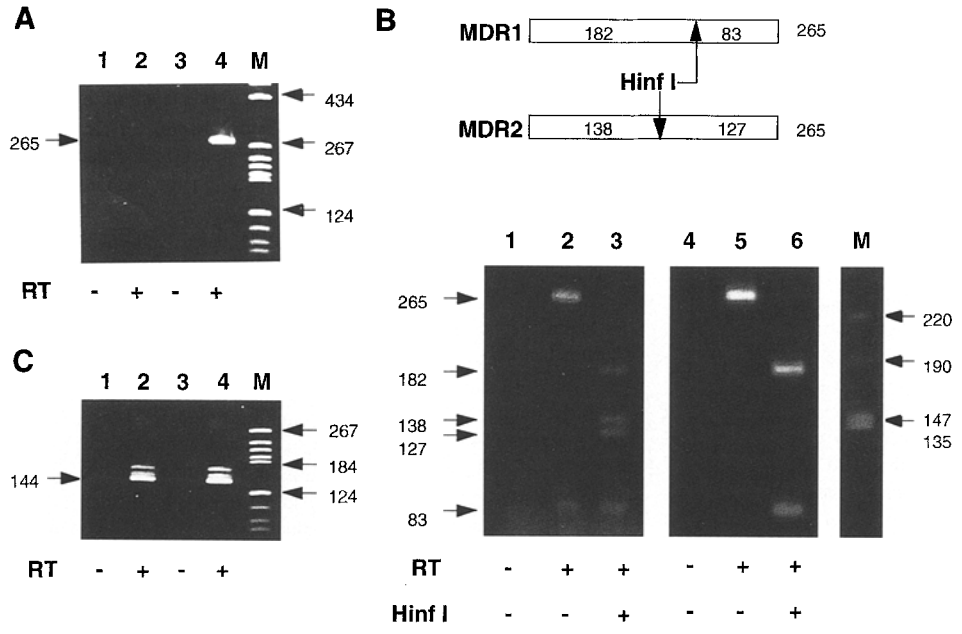

Fig. 1. RT-PCR analysis of MDR-1 Pgp expression in K562 and K562 VBL400 cells. (*A*) Ethidium bromide stained gel of MDR-1/2 RT-PCR products in K562 and K562 VBL400 cells (*see* Materials and Methods). Lanes 1 and 2: K562; lanes 3 and 4: K562 VBL400; lane M: markers; the + and – signs refer to the presence or absence of reverse transcriptase (*RT*) during the first strand cDNA synthesis step. Note the prominent 265 nt MDR-1/2 band in K562 VBL400 but not in K562. (*B*) PhosphorImager analysis of MDR-1/2 RT-PCR products in K562 and K562 VBL400. Aliquots of the PCR products shown in panel *A* were diluted into a second PCR mix that contained 2.5 μCi dCTP[α-^{32}P] and amplified as described (*see* Materials and Methods). Lanes 1 to 3: K562; lanes 4 to 6: K562 VBL400; lane M: markers. The + and – signs refer to the presence or absence of reverse transcriptase (*RT*) during the first strand cDNA synthesis step or to the inclusion or exclusion of a Hinf I digestion after the PCR reaction (*see* Results). Note that the intensity of the signals in lanes 1–3 (K562) was enhanced relative to that in lanes 4–6 (K562 VBL400) to allow photographic reproduction. In K562 a band of approximately 85 nt was already present before Hinf I digestion (lane 2). This 'ghost' band partially obscures the MDR-1 derived 83 nt band in lane 3. (*C*) Control RT-PCR experiment, using primers for actin (*see* Materials and Methods). A 144 nt band of comparable intensity was amplified in both cell lines. Lanes 1 and 2: K562; lanes 3 and 4: K562 VBL400; the + and – signs refer to the presence or absence of reverse transcriptase during the first strand cDNA synthesis step.

with Hinf I allows discrimination between MDR-1-specific and MDR-2-specific fragments. On gels stained with ethidium bromide we could easily detect after 32 PCR cycles a 265 nt MDR-1/2 fragment in K562 VBL400 but not in K562 cells (Fig. 1*A*). We then radioactively labeled the PCR products by diluting an aliquot in a fresh PCR mix containing dCTP[α-^{32}P] and performing 10 additional cycles (*see* Materials and Methods). The amplified bands were digested with Hinf I and analyzed on a PhosphorImager after gel electrophoresis. The restriction pattern of the 265 nt band (Fig. 1*B*) indicates that, in K562 VBL400 cells, this band is nearly exclusively derived from MDR-1 (182 and 83 Hinf I fragments). Using this sensitive method, we could also observe a faint 265 nt MDR-1/2 band in parental K562 cells (Fig. 1*B*) which, on the basis of the restriction enzyme pattern, consisted of a mixture of MDR-1 (182 and 83 Hinf I) and MDR-2 (138 and 127 nt) fragments. These results indicate that K562 cells also express MDR-1 Pgp, albeit at a much lower level. Finally we checked the quality and the integrity of the RNA samples by performing a PCR analysis of actin on the same RT mixtures that had been used for MDR-1 amplification. Figure 1*C* shows that a 144 nt actin fragment of comparable intensity could be amplified in both cell lines.

The RT-PCR analysis was complemented at the protein level by immunofluorescence analysis of MDR-1 Pgp expression. To this end, K562 and K562 VBL400 cells were incubated with either MRK16, a monoclonal antibody raised against an extracellular epitope of MDR-1 Pgp (Hamada and Tsuruo, 1987), or an isotypic control antibody that does not recognize a cell surface antigen in these cells. After incubation with a secondary, phyco-erythrin conjugated antibody, the presence of MDR-1 Pgp on the cell surface was evaluated with a FACS flow cytometer. The FACS profiles in Fig. 2 clearly show that K562 VBL400 cells overexpress Pgp as compared to the parental K562 cells. In fact, Pgp expression in K562 could not be detected using this method as the MRK16 curve coincided with the control curve, obtained with an isotypic antibody. The lack of detection of Pgp in parental K562 cells by flow cytometry, but labeled with a different monoclonal antibody (C219), agrees with a recent report (Hait et al., 1993). These data suggest that membrane levels of Pgp in parental K562 cells are indeed very low.

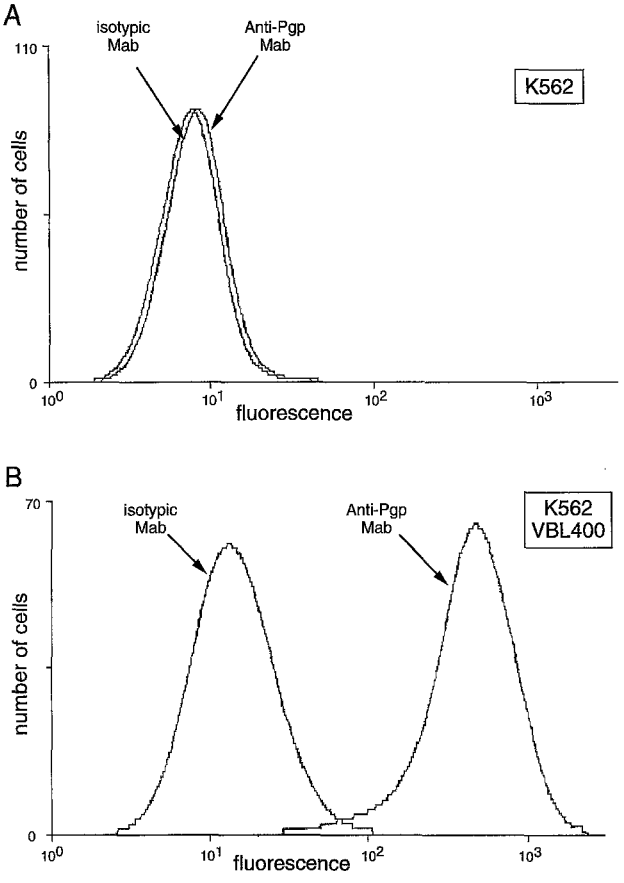

Fig. 2. FACS analysis of MDR-1 Pgp expression in K562 and K562 VBL400. Expression of Pgp at the cell surface was determined with MRK16, a monoclonal antibody against Pgp. Control curves were obtained by labeling the cells with an isotypic monoclonal antibody. Binding of MRK16 or the control antibody to the cells was measured by FACS analysis. *A* and *B* show the FACS profiles for K562 and K562 VBL400, respectively. Note that for K562 cells the MRK16 curve superimposes on the control curve whereas in K562 VBL400 cells the MRK16 curve is shifted to the right indicating significant expression of Pgp.

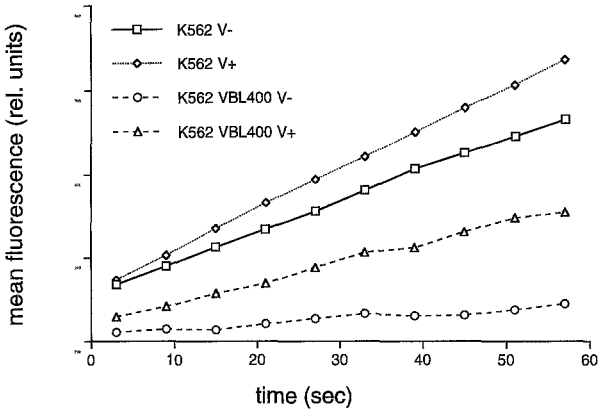

Fig. 3. Pgp-mediated transport in K562 and K562 VBL400. Time course of Fluo3 accumulation in K562 and K562 VBL400 in the presence (V+) or absence (V–) of 20 μM verapamil. Cells were incubated with Fluo3-AM and the intracellular accumulation of Fluo3 was monitored by measuring the mean channel fluorescence with a FACS flow cytometer. Experiments were performed in the absence or presence of verapamil (20 μM) which blocks Pgp mediated transport. The data are derived from one experiment and are representative of those obtained in three other experiments.

Differences in Pgp-mediated Transport between K562 and K562 VBL400 Cells

We also investigated whether we could detect any differences in Pgp-mediated transport between these two cell lines. To do so, we took advantage of the fact that hydrophobic acetoxymethyl ester fluorescent dyes such as Fluo3-AM, are substrates for the Pgp transport system (Homolya et al., 1993). Hence, when cells are incubated with Fluo3-AM, passive diffusion of the dye into the cell is counteracted by extrusion of the dye by the Pgp transport system. The intracellular accumulation of Fluo3-AM and consequently of the hydrolyzed Fluo3 is therefore inversely proportional to the Pgp transport capacity. We measured Fluo3 accumulation in K562 and K562 VBL400 by monitoring the mean channel fluorescence as a function of time with a FACS flow cytometer (Fig. 3). K562 cells gradually accumulate Fluo3 as indicated by the increase in cell-associated fluorescence with time. 20 μM verapamil, an inhibitor of Fluo3-AM transport by Pgp (Homolya et al., 1993), slightly increases the rate of fluorescence accumulation in the parental K562 cell line, indicating a small but demonstrable Pgp transport activity. In contrast, K562 VBL400 cells hardly accumulate any Fluo3 as indicated by the nearly flat slope of the curve in Fig. 3. Furthermore, addition of verapamil clearly increases the slope of the accumulation curve which reflects the contribution of Pgp to Fluo3-AM extrusion.

Induction of an Ionic Current by Hypotonicity

The traces in Fig. 4*A* show a series of currents in a K562 vinblastine resistant cell (K562 VBL400). These currents were evoked by voltage ramps from −100 to +100 mV at different times after switching the bath to hyposmotic solution. An outwardly rectifying current began to develop within seconds of the solution exchange. Figure 4*B* shows the time course of current development, measured at two different potentials. The filled circles plot the mean current for a voltage window between +75 and +85 mV, while the filled squares plot the mean current for a voltage window between −85 and −75 mV. Current develops earlier at depolarized potentials and has a larger amplitude. The degree of reversibility during return to isosmotic solution showed a marked variability, from nearly complete recovery (*see* Fig. 7*B*) to no recovery. However, application of hyperosmotic external solution caused an almost complete recovery in the majority of cells (Fig. 4*B* and *D*). A second hypotonic challenge was

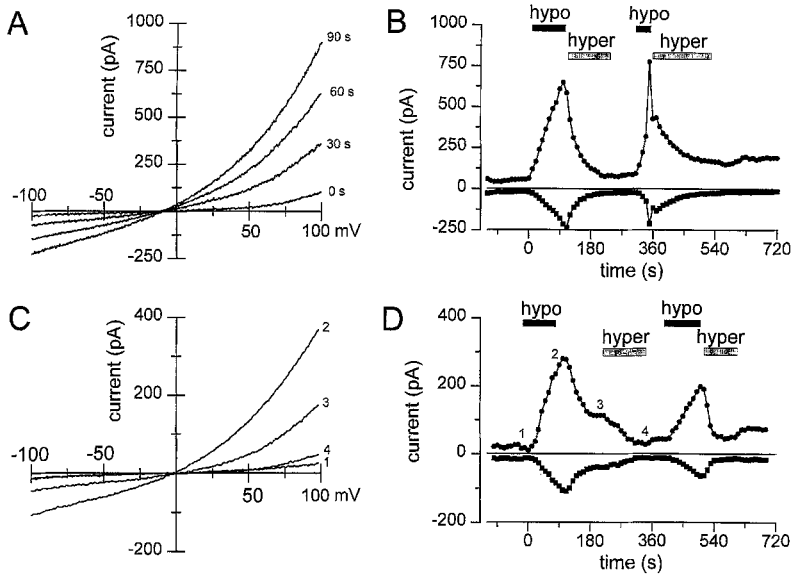

Fig. 4. Transmembrane osmotic gradients activate identical ionic conductances in K562 and K562 VBL400 cells. (*A*) Series of whole-cell currents elicited by voltage ramps (−100 to +100 mV), delivered every 10 sec in a K562 VBL400 cell. Next to each sweep is the time elapsed since the start of perfusion with hyposmotic extracellular solution. (*B*) Time course of the hyposmotic-induced current (same cell as in *A*). Circles and squares represent the mean current measured during a 10 mV window centered at +80 and −80 mV respectively. Note the larger current amplitude at +80 mV. The peak current during the second hyposmotic challenge is contaminated by transient activation of a calcium-dependent potassium current. (*C*) Whole-cell currents in a parental K562 cell (same protocol as in *A*) at different times during an hyposmotic challenge. Numerals to the right of the traces correspond to the times labeled in *D*. (*D*) Time course of the swelling-sensitive current (same sampling periods as in *C*). Note the partial recovery of current upon return to isosmotic conditions and the additional recovery during external hyperosmotic recordings. The smaller currents in *C* and *D* compared to those in *A* and *B* reflect only the large range of current amplitudes measured in these cells.

able to induce an increase in current, often of smaller amplitude than during the first hyposmotic challenge. Currents evoked by hyposmotic stimulation were nearly identical in parental K562 cells compared to those evoked in K562 VBL400 cells. An example of currents measured in a representative parental K562 cell at different times during an hyposmotic stimulus is shown in Fig. 4*C*, and the time course of current development is shown in Fig. 4*D*.

Figure 5*A* and *B* show bar histograms of current density (10 pA/pF bins) of the swelling-activated current in K562 and K562 VBL400 cells, respectively. There was a great variability in current densities for individual cells in both populations. In a significant number of cells exposure to hyposmotic solution did not activate a current (*not shown*). The proportion of nonresponding cells did not differ between the parental (K562) and the drug-selected (K562 VBL400) cell lines: in the K562 population 23.7% of the cells did not respond.[1] For the K562 VBL400 population this percentage was 22.7%. The mean current density of the responding K562 cells (39.6 ± 4.9 pA/pF; $n = 29$) was not significantly different from the mean current density in the responding K562

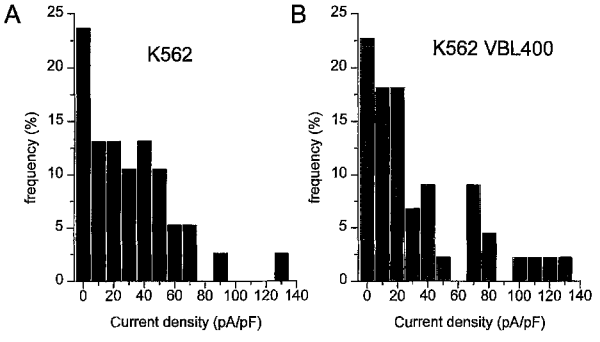

Fig. 5. Current densities of swelling-induced currents in K562 and K562 VBL400 cells. (*A*) Bar histogram of the current density distribution of swelling-induced currents in K562 cells. (*B*) The same histogram for K562 VBL400 cells. The first bar in both histograms represents the percentage of nonresponsive cells ($I_{Cl^-} < 5$ pA/pF).

VBL400 cells (41.7 ± 6 pA/pF; $n = 34$). The average cell capacitance was 10.9 ± 0.5 pF in parental cells compared to 12.5 ± 0.6 pF in drug-selected cells. This difference in average cell capacitance was statistically significant. Surprisingly, no current was induced in K562 (4 out of 4) or K562 VBL400 (3 out of 4) cells when recorded in the perforated whole-cell configuration (*not shown*). In contrast, HeLa cells showed large and readily reversible volume-activated currents when recorded under identical

[1] We defined nonresponsive cells as those having a volume-sensitive current density smaller than 5pA/pF, measured at +80 mV.

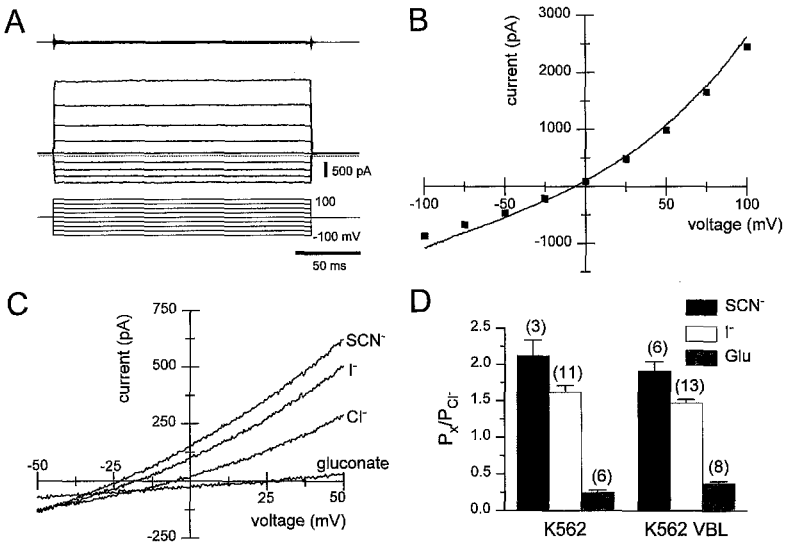

Fig. 6. Gating and permeation properties of the swelling-induced Cl^- conductance. (*A*) Current responses to 200 msec duration hyperpolarizing and depolarizing voltage steps in a parental K562 cell held at 0 mV. The top trace shows records in isosmotic solution and the middle trace records from the same cell in hyposmotic solution. The dotted line represents the zero current level. No leak or capacitive current subtraction. (*B*) Current-voltage relationship of the whole-cell current recorded in hyposmotic conditions for the same cell as in *A*. The filled squares represent current measured 10 msec after the beginning of the voltage pulse and the continuous line, current obtained from a 1-sec duration voltage ramp. (*C*) Swelling-induced ramp currents in a K562 VBL400 cell, recorded after replacing extracellular Cl^- with gluconate, I^- and SCN^-. Records have been subtracted from a background ramp current recorded in isosmotic solution. (*D*) Plot of relative permeabilities for different extracellular anions in K562 parental and K562 VBL400 cells (*see* Materials and Methods).

conditions (2 out of 2) (*not shown*) (*see also* Nilius, Sehrer & Droogmans, 1994). We will show below that these currents are carried by chloride primarily.

Gating of Volume-Sensitive Cl^- Channels

The gating of volume-activated Cl^- channels in K562 cells lacked significant voltage dependence. Figure 6*A* shows current responses in a parental K562 cell to voltage steps in isosmotic (top panel) and in hyposmotic (middle panel) conditions. The swelling-induced current activates very fast and is nearly constant during the 200 msec duration steps from −100 to +100 mV. At +50 mV the current inactivated by 5 ± 2% (n = 4), while inactivation at +100 mV was 8 ± 4% (n = 4). Deactivation kinetics were also very fast, with no detectable tail currents. Plotted in Fig. 6*B* are current values measured 10 msec after the start of the voltage steps (filled squares) and the current response to a 1-sec voltage ramp, delivered a few seconds after applying the step protocol. The degree of outward rectification obtained during voltage steps matches closely the one observed during voltage ramps. Furthermore, these records were obtained in symmetrical internal and external chloride (105 mM NMDGCl inside *vs.* 105 mM NaCl outside), suggesting that outward rectification in volume-sensitive chloride channels is due to permeation properties rather than to voltage- or time-dependent gating.

Permeation Properties and Pharmacology of the Swelling-Induced Current

The current could be induced in cells recorded with either Cs^+ or K^+ as the main intracellular cation, suggesting that it is not a K^+ current. In symmetrical chloride solutions and with NMDG inside and Na^+ outside, it reversed at −5 ± 1 mV (n = 3) suggesting that it is not a nonselective cation current. With the standard intracellular solution the current reversed at −9.2 ± 1.5 mV (n = 17) in K562 and −11.4 ± 0.6 mV (n = 22) in K562 VBL400 cells (E_{Cl^-} = −25 mV). A significant deviation from the Cl^- equilibrium potential was previously noted for volume-sensitive chloride currents of other cell types, like T lymphocytes (Lewis, Ross & Cahalan, 1993) or retinal pigment epithelium (Botchkin & Matthews, 1994) and partially explained by significant permeability to aspartate, the main intracellular anion in our experiments. Assuming a relative permeability to aspartate of 0.2 with respect to chloride, the estimated reversal potential would be −15 mV for our recording conditions.

Different chloride currents have a particular anion selectivity sequence. To investigate the relative permeabilities of the current activated by hypotonicity we replaced extracellular Cl^- with different anions and measured the shift in reversal potential. Examples of ramp currents obtained in the same K562 VBL400 cell in the presence of sodium salts of Cl^-, SCN^-, I^- and gluconate are shown in Fig. 6*C*. Chloride was more permeable than gluconate but less than iodide or SCN^-. The permeability ratios for different anions are illustrated separately for K562 and K562 VBL400 cells in the Fig. 6*D*. There were no significant differences in the permeability ratios of the two cell lines, suggesting that hypotonicity induces a similar anion current in K562 and K562 VBL400 cells.

The osmotically activated current was blocked by the chloride channel blocker NPPB as shown in Fig. 7*A*. Shown in this K562 cell are current responses to voltage ramps in control (isosmotic solution), following hypos-

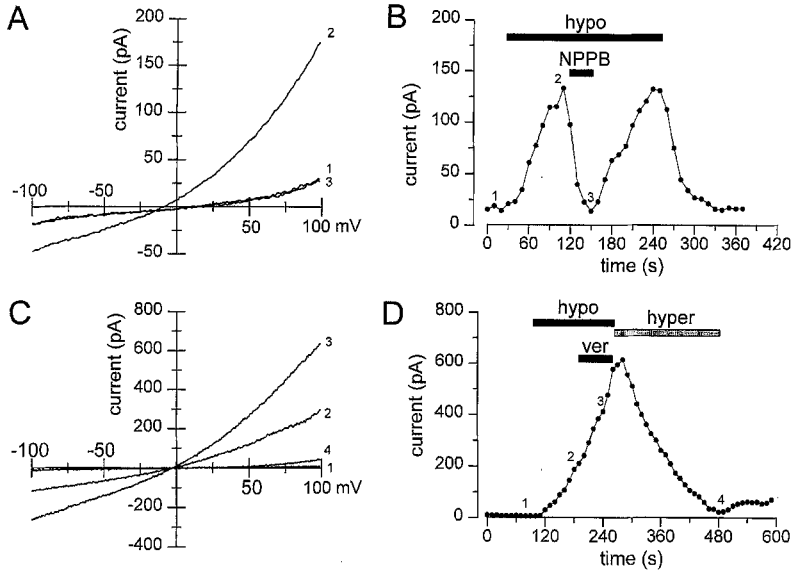

Fig. 7. Pharmacology of swelling-induced currents. (*A*) Ramp currents recorded in a parental K562 cell in isosmotic solution, during an hyposmotic challenge (hypo) and during the application of 100 μM NPPB, in the continuous presence of hyposmotic solution. (*B*) Full time course of the average current (10 mV window centered around +80 mV). Same cell as *A*. (*C*) Ramp currents recorded in a K562 VBL400 cell in control isosmotic solution, in hyposmotic solution and after addition of 100 μM verapamil. (*D*) Time course of current development. Same cell as in *C*.

motic replacement and during application of 100 μM NPPB. In this case, block was complete and rapidly reversible upon wash. On average, the inhibition at +80 mV was 94 ± 3% ($n = 6$) for K562 cells and 90 ± 5% ($n = 6$) for K562 VBL400 cells. In contrast, verapamil (50 to 100 μM), an effective blocker of Pgp-associated Cl^- current (Valverde et al., 1992) and of Pgp-associated drug transport (*see* Fig. 3) did not inhibit the volume-activated current in K562 or K562 VBL400 cells ($n = 4$). Figure 7*C* shows current traces in a K562 VBL400 cell in isosmotic conditions and hyposmotic conditions, before and during application of 100 μM verapamil. In this particular example the current continued to increase, even during verapamil application, but returned to baseline during drug washout in hyperosmotic solution.

Hypotonicity Does not Affect Pgp Transport Capacity

A volume-activated Cl^- current has recently been associated with the MDR-1 molecule (Gill et al., 1992). A model was developed, proposing that channel and drug transport activities of P-glycoprotein reflect two different, mutually exclusive, functional states of the protein. The interconversion between the two states is mediated by changes in extracellular tonicity and by the availability of substrate. According to this proposal, incubation in hypotonic solution would switch the protein into its channel function mode. On the other hand, when the protein functions as transporter, channel function is excluded. We therefore wanted to test whether Pgp-mediated transport in K562 and K562 VBL400 cells is affected by the tonicity of the extracellular medium and also whether activation of a Cl^- current can be prevented by loading the cell with transport substrates such as vinblastine or vincristine in the presence of hydrolyzable ATP (*see* next section). These results are predicted by the bimodal transporter-channel function of Pgp (Gill et al., 1992).

Fluo3 accumulation in K562 VBL400 cells was studied in isotonic and hypotonic media with or without verapamil (20 μM), a blocker of P-glycoprotein mediated dye extrusion (Homolya et al., 1993). The contribution of Pgp to dye extrusion can therefore be inferred from the increase in fluorescence accumulation in the presence of 20 μM verapamil. As shown in Fig. 8*A* Fluo3 accumulation in K562 VBL400 was not affected by the tonicity of the extracellular medium as equal accumulation rates were obtained in isotonic and hypotonic media. Furthermore, addition of verapamil accelerated the Fluo3 accumulation in isotonic and in hypotonic medium to the same extent. Therefore, Pgp transporters were equally active in isotonic and hypotonic conditions indicating that Pgp-mediated transport in K562 VBL400 cells is not down regulated in hypotonic medium. One possible explanation for the lack of inhibition could be that as a result of the drug selection K562 VBL400 cells overexpressed a mutant Pgp that no longer responded to changes in extracellular tonicity. We therefore repeated the same experiments with the parental K562 cells (Fig. 8*B*) which have never been cultured in the presence of vinblastine. However, we observed qualitatively similar results in the parental cells, i.e., hypotonicity did not affect the accumulation rate of Fluo3 and verapamil increased the accumulation rate of Fluo3 to the same extent under isotonic and hypotonic conditions. Therefore, the lack of inhibition cannot be ascribed to a mutation in the Pgp molecule. An alternative explanation for the lack of inhibition could be that conversion from transporter mode to channel mode is not yet maximal at the time of transport measurement. We therefore repeated these experiments but waited 3 min instead of 30 sec between the hypotonic stimulus and the addition of Fluo3-AM after

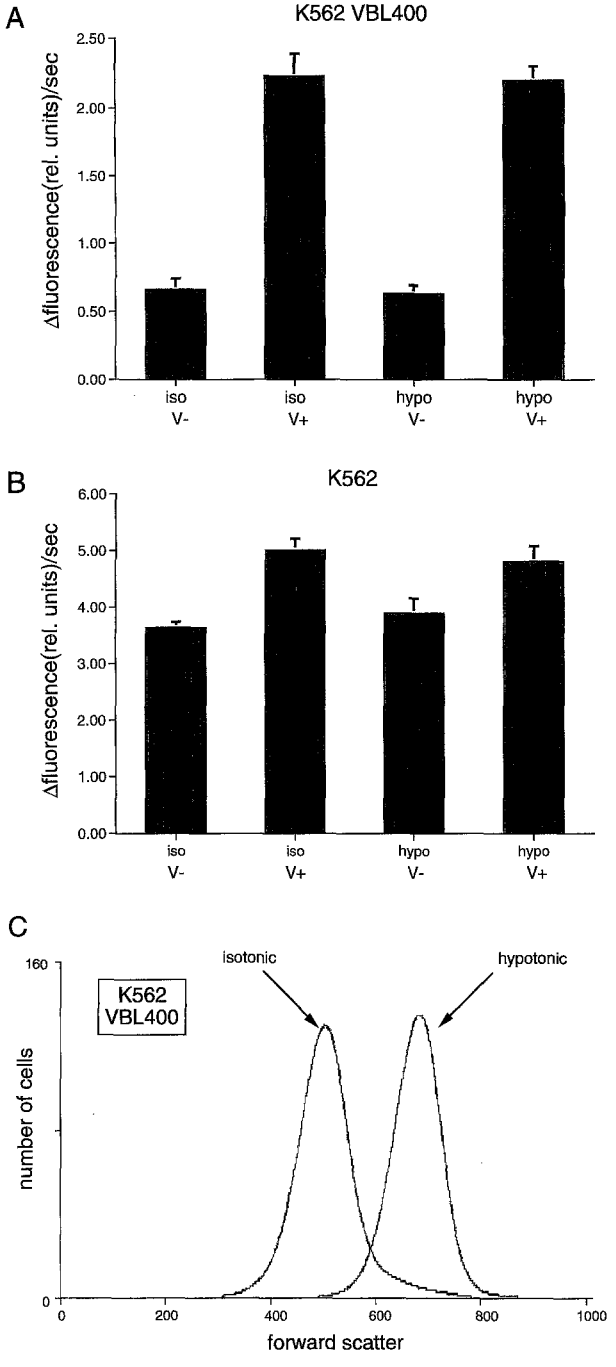

Fig. 8. Hypotonicity does not affect Pgp-mediated transport. Intracellular accumulation of Fluo3 was measured in isotonic (iso) and hypotonic (hypo) conditions. To reduce the tonicity of the extracellular medium, 80 μl of H_2O were added to 120 μl of cell suspension after which Fluo3-AM was added and transport measurement was started. Accumulation rates in both conditions were determined in the absence (V−) or presence (V+) of verapamil (20 μM) which blocks Pgp-mediated transport. *A* and *B* show the accumulation rates for K562 VBL400 and K562, respectively. Note that basal accumulation rates are identical in isotonic and hypotonic conditions and that verapamil is still able to accelerate uptake in both isotonic and hypotonic conditions. The mean values were derived from three experiments and the standard deviation for each condition is indicated above each bar. *C* is a distribution plot of the forward scatter of K562 VBL400 cells in isotonic and hypotonic medium. The increase in forward scatter in hypotonic medium is a reflection of change in cell size due to cell swelling.

which transport measurement was immediately started. Again, we obtained similar results independently of the time interval between hypotonic stimulation and addition of Fluo3-AM (*data not shown*). Therefore, time-dependent effects cannot account for the lack of transport inhibition by hypotonicity. Finally, we also verified whether these cells swell after hypotonic stimulation. Cell size can be estimated from the forward scatter measured by a FACS flow cytometer (Muirhead, Horan & Poste, 1985). Figure 8*C* shows an increase in forward scatter when the extracellular tonicity is reduced. This confirms that K562 VBL400 cells swell after hypotonic stimulation. We therefore conclude that in K562 and K562 VBL400 cells, Pgp-mediated transport is not affected by the extracellular tonicity.

Pgp Substrate Loading Does not Prevent Activation of Volume-sensitive Current

In MDR-1 transfected S1/1.1 lung carcinoma cells and NIH3T3 fibroblasts, Gill et al., (1992) showed that whole-cell recordings with pipettes containing ATP and various cytotoxic drugs (all substrates of Pgp-mediated transport) caused a large inhibition (>80%) of the volume-sensitive current. Therefore, we also tested whether activation of the volume-sensitive Cl^- current can be prevented by loading the cells with a substrate for the transporter in the presence of hydrolysable ATP. As shown in Fig. 9*A*, the protocol consisted in obtaining the whole-cell configuration with a pipette containing 250 μM vinblastine (or 250 μM vincristine) and waiting a period of 5 min before applying the hyposmotic solution. In most cases, the current (measured at +80 mV) showed a small and progressive increase during the isosmotic period. The amplitude and rate of current development increased rapidly in the presence of hyposmotic solutions and was reversed by hyperosmotic external solutions. The current was also sensitive to 100 μM NPPB. The same protocol with control pipettes yielded identical results (Fig. 9*B*), a progressive increase in current during isosmotic conditions followed by a rapid increase in hyposmotic solutions. The bar chart in Fig. 9*C* summarizes these results. In control cells the mean current density was 46 ± 7 pA/pF (n = 7), compared to 35 ± 7 pA/pF (n = 6) in vinblastine-loaded and 36 ± 9 in vincristine-loaded cells (n = 3). These differences were not statistically significant.

Discussion

Our results show that drug transport as measured by Fluo3 accumulation in K562 cells is correlated with the level of P-glycoprotein expression and blocked by known inhibitors of this transporter, e.g., verapamil. In addition, dye transport was not influenced by the tonicity

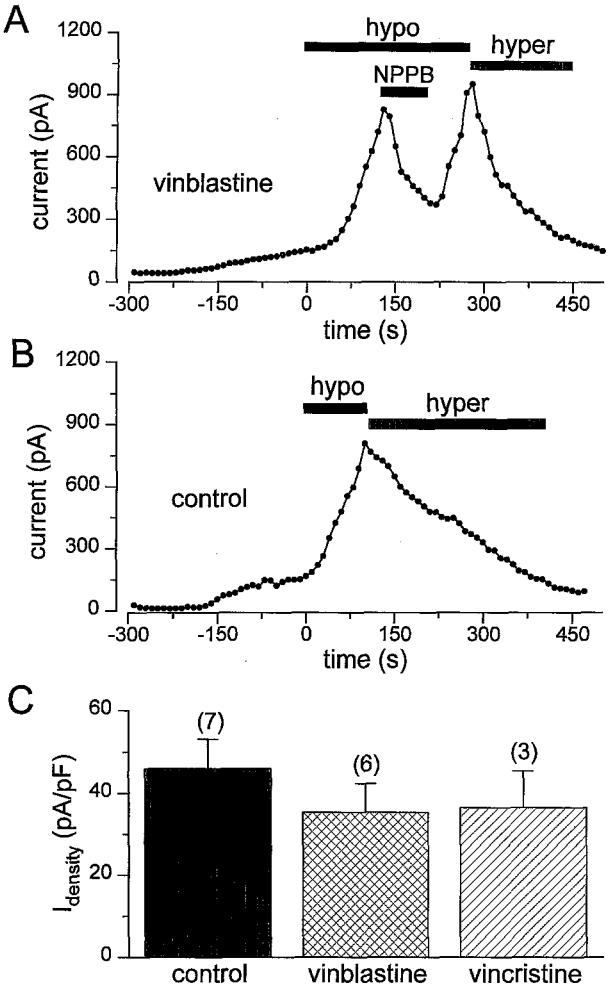

Fig. 9. Activation of swelling-sensitive current is insensitive to cytotoxic drugs. (*A*) Time course of current activation in a K562 VBL400 cell recorded with a pipette containing 250 μM vinblastine. Currents evoked by 1-sec linear ramps (−100 to +100 mV) and measured at +80 mV. Time zero corresponds to the start of the hyposmotic challenge. (*B*) Time course of current activation in a K562 VBL400 cell recorded with a control pipette (*see* Materials and Methods). (*C*) Bar histogram of average current (measured around +80 mV) in control cells (n = 7), vinblastine-loaded cells (n = 6) and vincristine-loaded cells (n = 3). A fourth cell loaded with vincristine did not respond to hyposmotic solution (I < 5 pA/pF).

of the extracellular medium. As expected, vinblastine-selected K562 cells overexpress MDR-1 Pgp and have a higher Pgp transport capacity than the parental K562 cells. In marked contrast to the drug transport data, the swelling-induced Cl^- current was not directly correlated with the level of P-glycoprotein expression as there were no significant differences between the swelling-induced Cl^- currents in K562 and K562 VBL400 cells. Furthermore, currents were not affected by preloading the cells with Pgp substrates.

The volume-activated chloride current in parental and drug-selected K562 cells shares several features with volume-activated chloride currents recently described in other cell types such as chromaffin cells (Doroshenko, Penner & Neher, 1991; Doroshenko & Neher, 1992), Jurkat T lymphocytes (Lewis et al., 1993), HeLa cells (Diaz et al., 1993), epithelial cells (Kubo & Okada, 1992), human endothelial cells (Nilius et al., 1994*a,b*) and a large sample of various nonexcitable cells (Nilius et al., 1994*c*). These currents share the following properties: (i) more permeable to iodide than to chloride; (ii) outwardly rectifying current-voltage relationship; (iii) potent and reversible block by 100 μM NPPB; (iv) small single-channel conductance of less than 5 pS (no data available for K562 cells).

The swelling-induced Cl^- currents in K562 cells, parental and drug-selected, displayed two intriguing features. First, a gradual spontaneous induction of the volume-activated Cl^- current can occur under isosmotic conditions in K562 and K562 VBL400 cells, and current reversibility from hyposmotic stimulus often requires perfusion with external hyperosmotic solutions. These observations are similar to those made previously for a volume-sensitive chloride conductance in the human colonic cell line T84 (Worrell et al., 1989), and suggest that some osmotically active macromolecules within the cell do not equilibrate readily with the pipette solution. In contrast, a complete reversibility and repeatability of Cl^- current responses to hyposmotic stimuli has been described in human endothelial cells (Nilius et al., 1994*a*). Second, a significant percentage of cells did not activate a conductance when challenged with a hyposmotic external solution. Similarly, no volume-sensitive currents were induced in about 20% of epithelial cells tested by Solc and Wine, 1991. Some of the unresponsive K562 cells could be activated by applying small positive intrapipette pressures. This discrepancy between the effectiveness of transmembrane osmotic gradients compared to changes in pipette pressure was previously noted by Lewis et al. (1993) in lymphocytes. In contrast to our own experience with endothelial cells (Nilius et al., 1994*a*), and HeLa cells (Nilius et al., 1994*b*), induction of the volume-sensitive conductance was not observed in K562 cells during perforated patch recordings. This result may indicate that a yet unidentified cytosolic constituent of K562 cells exerts an inhibitory effect upon the coupling of cell-swelling to channel gating, such that dialysis of the cell is required before channel activation can take place. Another extreme case of nonresponsiveness was reported recently for Chinese hamster lung fibroblasts (Altenberg et al., 1994). In that study, neither wild-type fibroblasts nor highly multidrug-resistant fibroblasts (overexpressing Pgp) showed a current induction by hyposmostic solutions. This variability in response to cell swelling is also interesting in light of the recent identification in *Xenopus* of an actin-bound cytosolic protein that can modulate a volume-sensitive chloride conductance (Krapivinsky et al., 1994).

Some properties of the swelling-activated Cl^- conductance in both parental and vinblastine-selected K562

cells matched more closely the properties of a chloride current in lymphocytes (Lewis et al., 1993) compared to the current described in transfected 3T3 fibroblasts (Valverde et al., 1992) and presumably associated with Pgp expression. For example, the current in transfected fibroblasts, as well as in some epithelial cell lines (Kubo & Okada, 1992; Rasola et al., 1994), displayed substantial time-dependent inactivation at positive potentials, whereas the K562 current did not. In addition, 100 μM verapamil inhibited the current in transfected fibroblasts (Valverde et al., 1992, Mintenig et al., 1994) but was ineffective in K562 cells and lymphocytes. Verapamil was also a poor blocker of the chloride current in drug-selected epithelial cell lines (Rasola et al., 1994) and of the hypotonicity-activated chloride current constitutively expressed in *Xenopus* oocytes (Ackerman et al., 1994).

An important question bearing on our data relates to the molecular identity of the volume-sensitive Cl^- current in K562 cells. It has been reported that NIH 3T3 fibroblasts and S1 lung cancer cells do not display a hypotonicity-activated Cl^- current unless they have been transfected with MDR-1 cDNA (Valverde et al., 1992). As mentioned, we did not detect any significant differences in the biophysical properties such as outward rectification, sensitivity to NPPB and permeability to anions, in the mean current density of the swelling-activated chloride current or in the percentage of responsive cells between K562 and K562 VBL400 in spite of the different MDR-1 expression levels. A similar lack of correlation between the size of swelling-induced Cl^- current and the level of P-glycoprotein expression has also been reported in cell lines derived from human colon adenocarcinoma and tracheal epithelium (Rasola et al., 1994). It could be argued that the lack of correlation is a consequence of the drug selection procedure. For example, drug selection could accidentally result in the overexpression of a mutant MDR-1 transporter that has lost its sensitivity to hypotonicity. Two observations argue against this: (i) the lack of correlation has been observed in three independently selected cell lines using two different drugs: K562 cells with vinblastine and LoVo (human colon adenocarcinoma) and $9HTE_o$- cells (human tracheal epithelial cells) with doxorubicin (Rasola et al., 1994); (ii) we have observed a similar lack of correlation between amplitude of volume-sensitive current and levels of Pgp expression while testing several mammalian cell lines that have never been exposed to cytotoxic drugs (De Greef et al., 1994).

Channel activation by hypotonic solutions was prevented in MDR-1 transfected cells when Pgp transport substrates such as vincristine were present prior to the hypotonic stimulus (Gill et al., 1992). In contrast, we found that addition of vinblastine or vincristine to the cell interior did not prevent the activation of volume-sensitive currents in K562 VBL400 cells. In agreement with our results, Altenberg et al. (1994) found that intracellular loading with rhodamine 123 (a substrate of Pgp) did not prevent activation of Cl^- currents by hyposmotic solutions in MDR-1 transfected human breast cancer cells. Similarly, loading human umbilical vein endothelial cells with hydrophobic substrates of P-glycoprotein did not prevent activation of volume-sensitive chloride currents (Nilius et al., 1994*b*). We also tested whether Pgp mediated transport in K562 was affected by the tonicity of the extracellular medium. One testable prediction of the model proposed by Gill et al. (1992) is that cells incubated in hypotonic medium should have a lower Pgp transport capacity. However, we did not find any effect of hypotonicity on the Pgp transport capacity in either the parental K562 or the K562 VBL400 cells. As we observed a similar effect in wild type and drug-selected K562 cells, it is very unlikely that the lack of effect can be ascribed to a mutation in Pgp due to the drug selection procedure. This result is in agreement with recent data from human breast cancer cells, where exposure to hyposmotic solutions did not alter rhodamine 123 efflux (Altenberg et al., 1994).

The lack of correlation between Pgp expression and the properties or the density of the volume-activated Cl^- current, the inability of Pgp substrates to affect current induction, the lack of modulation of Pgp transport by extracellular tonicity and the aforementioned differences between the Cl^- current in K562 cells and the MDR-1-associated chloride current in transfected fibroblasts suggest that in K562 cells the volume-activated current is unlikely to be associated with P-glycoprotein overexpression. We conclude that K562 cells express a volume-activated Cl^- channel that differs from the Pgp-associated Cl^- channel described in MDR-1 transfected S1 cells and NIH 3T3 fibroblasts. At the moment we do not know why overexpression of MDR-1 is related to a volume-activated Cl^- current in some cells, but not in others. Our data and the description of other chloride channels activated by hyposmotic challenges (Gründer et al., 1992) also hint to a diversity of volume-activated chloride conductances in eukaryotic cells, much in line with the diversity of other types of voltage and mechanically gated channels.

The authors wish to thank Dr. Humbert de Smedt, Ms. Anja Florizoone and Ms. Marina Crabbé for assistance in the culturing of cells. F.V. was supported by a post-doctoral fellowship (EX93 36037569) from the Ministerio de Educación y Ciencia (Spain). K.V.A. was supported by the Institute for Scientific Research in Agriculture and Industry (Belgium). J.E. is a postdoctoral fellow of the Belgian National Fund for Scientific Research (NFWO). C.D.G. and B.N. received support from the Max Planck Gesselschaft (Germany).

References

Ackerman, M.J., Wickman, K.D., Clapham, D.E. 1994. Hypotonicity activates a native chloride current in *Xenopus* oocytes. *J. Gen. Physiol.* **103:**153–179

Altenberg, G.A., Vanoye, C.G., Han, E.S., Deitmer, J.W., Reuss, L. 1994. Relationship between rhodamine 123 transport, cell volume,

and ion-channel function of P-glycoprotein. *J. Biol. Chem.* **269:**7145–7149

Block, M.L., and Moody, W.J. 1990. A voltage dependent chloride current linked to the cell cycle in ascidian embryos. *Science* **247:**1090–1092

Bormann, J., Hamill, O.P., Sakman, B. 1987. Mechanism of anion permeation through channels gated by glycine and γ-aminobutyric acid in mouse cultured spinal neurones. *J. Physiol.* **385:**243–286

Botchkin, L.M., Matthews, G. 1993. Chloride current activated by swelling in retinal pigment epithelium cells. *Am. J. Physiol.* **265:**C1037–C1045

Bretag, A.H. Muscle chloride channels. 1987. *Physiol. Rev.* **67:**618–725

Chomczynski, P., Sacchi, N. 1987. Single-step method of RNA isolation by acid guanidinium thiocyanate-phenol-chloroform extraction. *Anal. Biochem.* **162:**156–159

Cole, S.P.C., Bhardwaj, G., Gerlach, J.H., Mackie, J.E., Grant, C.E., Almquist, K.C., Stewart, A.J., Kurz, E.U., Duncan, A.M.V., Deeley, R.G. 1992. Overexpression of a transporter gene in a multidrug-resistant human lung cancer cell line. *Science* **258:**1650–1654

De Greef, C., Viana, F., Sehrer, J., Droogmans, G., Eggermont, J., Raeymaekers, L., Nilius, B. 1994. Expression of MDR-1 and MDR-2 in various cell types and the possible relation to volume-activated Cl^- channels. *Pfluegers Arch.* **427:**R59

Diaz, M., Valverde, M.A., Higgins, C.F., Rucareanu, C., Sepulveda, F.V. 1993. Volume-activated chloride channels in HeLa cells are blocked by verapamil and dideoxyforskolin. *Pfluegers Arch.* **422:**347–353

Doroshenko, P., Neher, E. 1992. Volume-sensitive conductance in bovine chromaffin cell membrane. *J. Physiol.* **449:**197–218

Doroshenko, P., Penner, R., Neher, E. 1991. A novel chloride conductance in the membrane of bovine chromaffin cells activated by intracellular GTPγS. *J. Physiol.* **436:**711–724

Endicott, J.A., Ling, V. 1989. The biochemistry of P-glycoprotein mediated multidrug resistance. *Ann. Rev. Biochem.* **58:**137–171

Frizzell, R.A., Halm, D.R. 1990. Chloride channels in epithelial cells. *Curr. Top. Membr. Transp.* **37:**247–282

Gill, D.R., Hyde, S.C., Higgins, C.F., Valverde, M.A., Mintenig, G.M., Sepulveda, F.V. 1992. Separation of drug transport and chloride channel functions of human multidrug resistance P-glycoprotein. *Cell* **71:**23–32

Grinstein, S., Foskett, J.K. 1990. Ionic mechanisms of cell volume regulation in leukocytes. *Ann. Rev. Physiol.* **52:**399–414

Gründer, S., Thiemann, A., Pusch, M., Jentsch, T.J. 1992. Regions involved in the opening of ClC-2 chloride channel by voltage and cell volume. *Nature* **360:**759–762

Hait, W.N., Choudhury, S., Srimatkandada, S., Murren, J.R. 1993. Sensitivity of K562 human chronic myelogenous leukemia blast cells transfected with a human multidrug resistance cDNA to cytotoxic drugs and differentiating agents. *J. Clin. Invest.* **91:**2207–2215

Hamada, H., Tsuruo, T. 1987. Functional role for the 170- to 180-kDa glycoprotein specific to drug-resistant tumor cells as revealed by monoclonal antibodies. *Proc. Nat. Acad. Sci. USA* **83:**7785–7789

Hoffmann, E.K., Simonsen, L.O. 1989. Membrane mechanisms in volume and pH regulation in vertebrate cells. *Physiol. Rev.* **69:**315–382

Homolya, L., Holló, Z., Germann, U., Pastan, I., M. Gottesman, M.M., Sarkadi, B. 1993. Fluorescent cellular indicators are extruded by the multidrug resistance protein. *J. Biol. Chem.* **268:**21493–21496

Horn, R., Marty, A. 1988. Muscarinic activation of ionic currents measured by a new whole-cell recording method. *J. Gen. Physiol.* **92:**145–159

Jentsch, T.J. 1993. Chloride channels. *Curr. Opin. Neurobiol.* **3:**316–321

Jirsch, J., Deeley, R.G., Cole, S.P.C., Stewart, A.J., Fedida, D. 1993. Inwardly rectifying K^+ channels and volume-regulated anion channels in multidrug-resistant small cell lung cancer cells. *Cancer Res.* **53:**4156–4160

Krapivinsky, G.B., Ackerman, M.J., Gordon, E.A., Krapivinsky, L.D., Clapham, D.E. 1994. Molecular characterization of a swelling-induced chloride conductance regulatory protein, pl_{Cln}. *Cell* **76:**439–448

Kubo, M., Okada, Y. 1992. Volume-regulatory Cl^- channel currents in cultured human epithelial cells. *J. Physiol.* **456:**351–371

Lewis, R.S., Ross, P.E., Cahalan, M.D. 1993. Chloride channels activated by osmotic stress in T lymphocytes. *J. Gen. Physiol.* **101:**801–826

Mintenig, G.M., Valverde, M.A., Sepulveda, F.V., Gill, D.R., Hyde, S.C., Higgings, C.F. 1994. Specific inhibitors distinguish the chloride channel and drug transporter functions associated with the human multidrug resistance P-glycoprotein. *In:* Receptors and Channels **1:**305–313

Muirhead, K.A., Horan, P.K., Poste, G. 1985. Flow cytometry: present and future. *Bio/Technology* **3:**337–356

Nilius, B., Oike, M., Zahradnik, I., Droogmans, G. 1994*a*. Activation of Cl^- channels by hypotonic stress in human endothelial cells. *J. Gen. Physiol.* **103:**787–806

Nilius, B., Sehrer, J., Droogmans, G. 1994*b*. Permeation properties and modulation of volume-activated Cl^--currents in human endothelial cells. *Brit. J. Pharmacol.* **112:**1049–1056

Nilius, B., Sehrer, J., Viana, F., De Greef, C., Raeymaekers, L., Eggermont, J., Droogmans, G. 1994*c*. Volume-activated Cl^- currents in different mammalian nonexcitable cell types. *Pfluegers Arch.* **428:**364–371

Oike, M., Droogmans, G., Nilius, B. 1994. Mechanosensitivity of endothelial cells is mediated by arachidonic acid. *Proc. Natl. Acad. Sci. USA* **91:**2940–2944

Paulmichl, M., Gschwentner, M., Wüll, E., Schmarda, A., Ritter, M., Kanin, G., Ellemunter, H., Waitz, W., Deetjen, P. 1993. Insight into structure-function relation of chloride channels. *Cell. Physiol. Biochem.* **3:**374–387

Paulmichl, M., Li, Y., Wickman, K., Ackerman, M., Peralta, E., Clapham, D. 1992. New mammalian chloride channel identified by expression cloning. *Nature* **356:**238–241

Rasola, A., Galietta, L.J.V., Gruenert, D.C., Romeo, G. 1994. Volume-sensitive chloride currents in four epithelial cell lines are not directly correlated to the expression of the MDR-1 gene. *J. Biol. Chem.* **269:**1432–1436

Solc, C.K., Wine, J.J. 1991. Swelling-induced and depolarization-induced Cl^- channels in normal and cystic fibrosis epithelial cells. *Am. J. Physiol.* **261:**C658–C674

Valverde, M.A., Diaz, M., Sepulveda, M., Gill, D.G., Hyde, S.C., Higgins, C.F. 1992. Volume regulated chloride channels are associated with the human multidrug-resistance P-glycoprotein. *Nature* **355:**830–833

Van Acker, K.L., Van Hove, L.M., Boogaerts, M.A. 1993. Evaluation of flow cytometry for multidrug resistance detection in low resistance K562 cells using daunorubicin and monoclonal antibodies. *Cytometry* **14:**736–746

Welsh, M.J. 1987. Electrolyte transport by airway epithelium. *Physiol. Rev.* **67:**1145–1184

Welsh, M.J., Smith, A.E. 1993. Molecular mechanisms of CFTR chloride channel dysfunction in cystic fibrosis. *Cell* **73:**1251–1254

Worrell, R.T., Butt, A.G., Cliff, W.H., Frizzell, R.A. 1989. A volume-sensitive chloride conductance in human colonic cell line T84. *Am. J. Physiol.* **256:**C1111–C1119